The SCWISh network is essential for survival under mechanical pressure - SI Appendix

M. Delarue[a,b], G. Poterewicz[b], O. Hoxha[a], J. Choi[a], W. Yoo[a], J. Kayser[a], L. Holt[b,†] and O. Hallatschek[a,†,*]

Name	Genotype	Provenance
BY4741	MATa his3Δ1 leu2Δ0 met15Δ0 ura3Δ0	Holt Lab
	[BY4741] WHI5::mCherry (URA3)	Thorner Lab
	[BY4741] ssk1Δ::HIS3	Thorner Lab
	[BY4741] sho1Δ::HISMX6	Holt Lab
	[BY4741] hkr1Δ::kanMX	Boeke Lab
	[BY4741] msb2Δ::kanMX	Boeke Lab
	[BY4741] ste11Δ::kanMX;WHI5::mCherry (URA3)	Hallatschek Lab
	[BY4741] kss1Δ::kanMX	Boeke Lab
	[BY4741] mid2Δ::kanMX	Boeke Lab
	[BY4741] mid2Δ::kanMX;slt2Δ::kanMX	Holt Lab
	[BY4741] bck1Δ::kanMX	Boeke Lab
	[BY4741] HOG1::mCherry (URA3)	Hallatschek Lab
	[BY4741] ssk1Δ::HIS3;HOG1::mCherry (URA3)	Hallatschek Lab
	[BY4741] sho1Δ::HIS3;HOG1::mCherry (URA3)	Holt Lab
	[BY4741] GFP::TUB1 (URA3)	Holt Lab
	[BY4741] msb2Δ::kanMX;GFP::TUB1 (URA3)	Holt Lab
	[BY4741] SLT2::GFP (HIS3)	Boeke Lab
	[BY4741] PKC1::GFP (HIS3)	Boeke Lab
	[BY4741] msb2Δ::kanMX;PKC1::GFP (HIS3)	Holt Lab
	[BY4741] mid2Δ::kanMX;PKC1::GFP (HIS3)	Holt Lab
	[BY4741] kss1Δ::HIS3;hog1Δ::kanMX	Thorner Lab
	[BY4741] ste11Δ::kanMX;slt2Δ::HIS3	Holt Lab

Table S1: Strains used in this study

*[1] Department of Physics and Integrative Biology, University of California, Berkeley, USA, [2] Institute for Systems Genetics, New York University Langone Medical Center, New York, USA, † These authors equally contributed to the work.

A parallelized device allows high throughput cell confinement

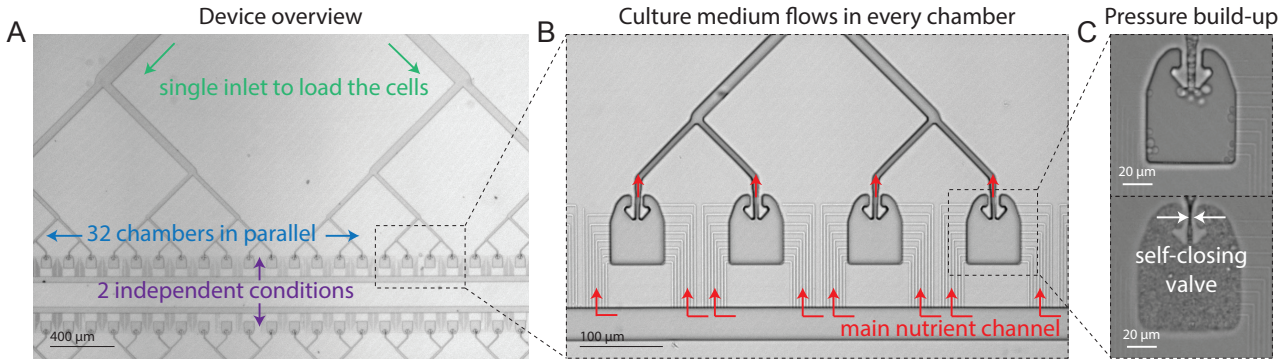

Figure S1: **a.** Overview of the parallel device. 32 parallel chambers are connected to a single inlet to load cells. The device is symmetric with a total of 2x32 chambers, allowing the definition of two independent conditions (in terms of cells or culture medium). **b.** Zoom on a series of 4 chambers. Each single chamber is connected to the main nutrient channel through a set of narrow channels: while the main chamber has a height of 10 μm, the smaller nutrient channels have a height of 0.5μm, thus these channels are too small for cells to enter. When cells are loaded in the device, culture medium flows through all the chambers, from the sides to the cell-inlet valve. **c.** Zoom on a single chamber, loaded with a few *S. cerevisiae* cells. When cells grow, they eventually fill the whole chamber. The cell-inlet channel is slightly smaller than individual cells, leading to jamming at the inlet [1]. The cells then fill the side-pockets, and deform the self-closing valve leading to full confinement of the cell population.

Pressure measurement and device calibration

Images were analyzed to define the chamber outline. The deformation of the chamber was then measured. Finite element simulations (Comsol) were performed with the geometry of the device presented on Fig. S5 (similar conclusions and calibration is drawn for the device presented on Fig. S1) with different Young's moduli - PDMS was defined as a hyperelastic material, as in [2]. We find a linear calibration relationship between the deformation and the imposed simulated pressure (Fig. S2a), which is used to experimentally determine the PDMS Youngâ€™s modulus, thereby fully calibrating our devices (Fig. S2b). This calibration is valid for both devices presented in this manuscript (Fig. S1 and S4), and enables us to measure the pressure developed in the chamber through its deformation.

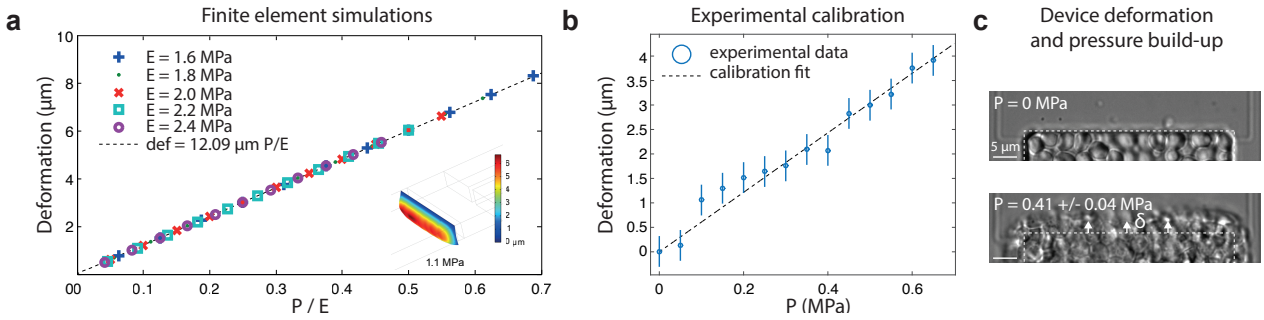

Figure S2: **a.** Finite element simulations define a linear relationship between pressure and chamber deformation as a function of the Young modulus of the PDMS composing the device. Inset: an example of the chamber deformation in the simulations for a pressure P = 1.1 MPa. **b.** We imposed a known water-driven pressure and measure the deformation of the chamber to calibrate our device. In this example, we measured a calibration for the deformation/pressure relationship of $6.1 \pm 0.3 \mu$m/MPa, which leads to a Young modulus $E = 1.98 \pm 0.11$MPa. We find that on average, our PDMS formulation yields a Young modulus around 2 MPa. **c.** Example of device deformation by growth-induced pressure. In this example, the deformation of the device is $\delta = 2.5 \pm 0.3 \mu$m, which, based on the calibration curve, corresponds to a cell population pressure of $P = 0.41 \pm 0.04$ MPa.

Cell size decreases under compressive stress

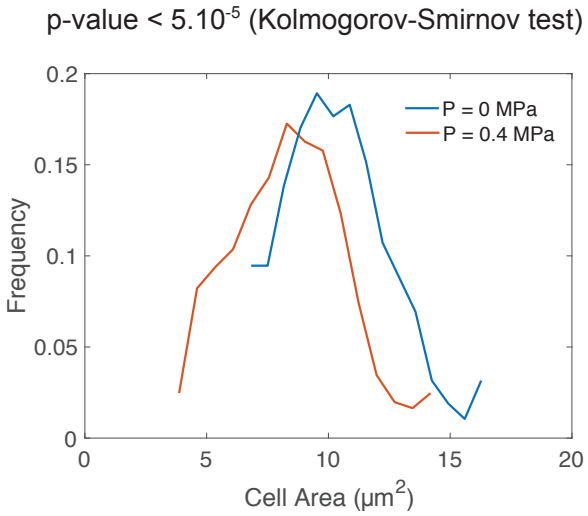

Figure S3: We measured cell area for ≥ 50 cells and plotted their distribution for P = 0 MPa and P = 0.4 MPa. Because cells are confined and compressed in all directions, cell area is a good proxy for cell size. We observe a 20% decrease in the mean cell area. A Kolmogorov-Smirnov test, assessing the statistical difference between the 2 distributions, returns that the 2 distributions are statistically different with a p-value $< 5.10^{-5}$.

Deletion of *SHO1* leads to cell death under compressive mechanical stress but not under compressive osmotic stress

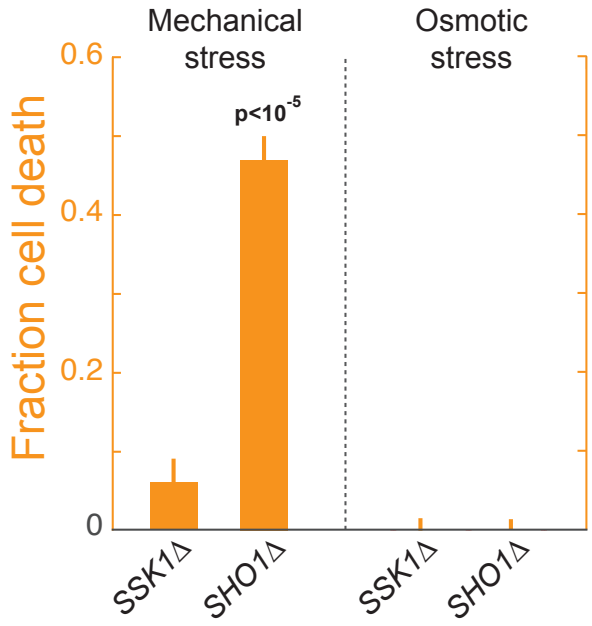

Figure S4: Change in cell death observed in *ssk1*Δ and *sho1*Δ cells, for both a mechanical stress of 0.4 MPa, and an osmotic stress (1M sorbitol). We did not observe an increase in cell death in the osmotic stress condition.

Microfluidic device to confine and instantaneously compress a cell population

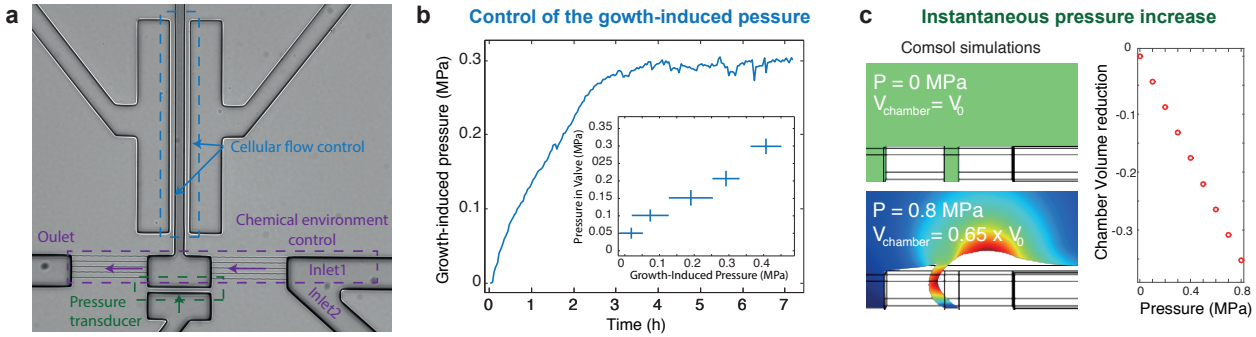

Figure S5: **a.** The device is composed of three main elements: a valve to control cell outflow and pressure build-up (blue element), two inlets to control the chemical environment and feed the cells through narrow channels, of the same geometry as in Fig. S1 (purple element), and a "micropiston" pressure transducer that enable instantaneous control of compressive mechanical stress (green element). **b.** When the valve is closed, cells are partially confined and build-up growth induced pressure. Pressure can be measured by determining the amount of pressure that must be applied to the pressure transducer to keep the membrane flat (more details in [1]. Inlet: the intensity of pressure build-up depends on the pressure imposed on the valve: the more closed the valve is, the higher the growth-induced pressure. **c.** The pressure transducer can be actuated to instantaneously compress the cell population. Finite element simulations (Comsol) show a transverse slice of the device when water-pressure is applied to deform the pressure transducer. The higher the pressure on the valve, the more the chamber volume decreases.

Extracting cell cycle stage from spindle shape in *GFP-TUB1* strains.

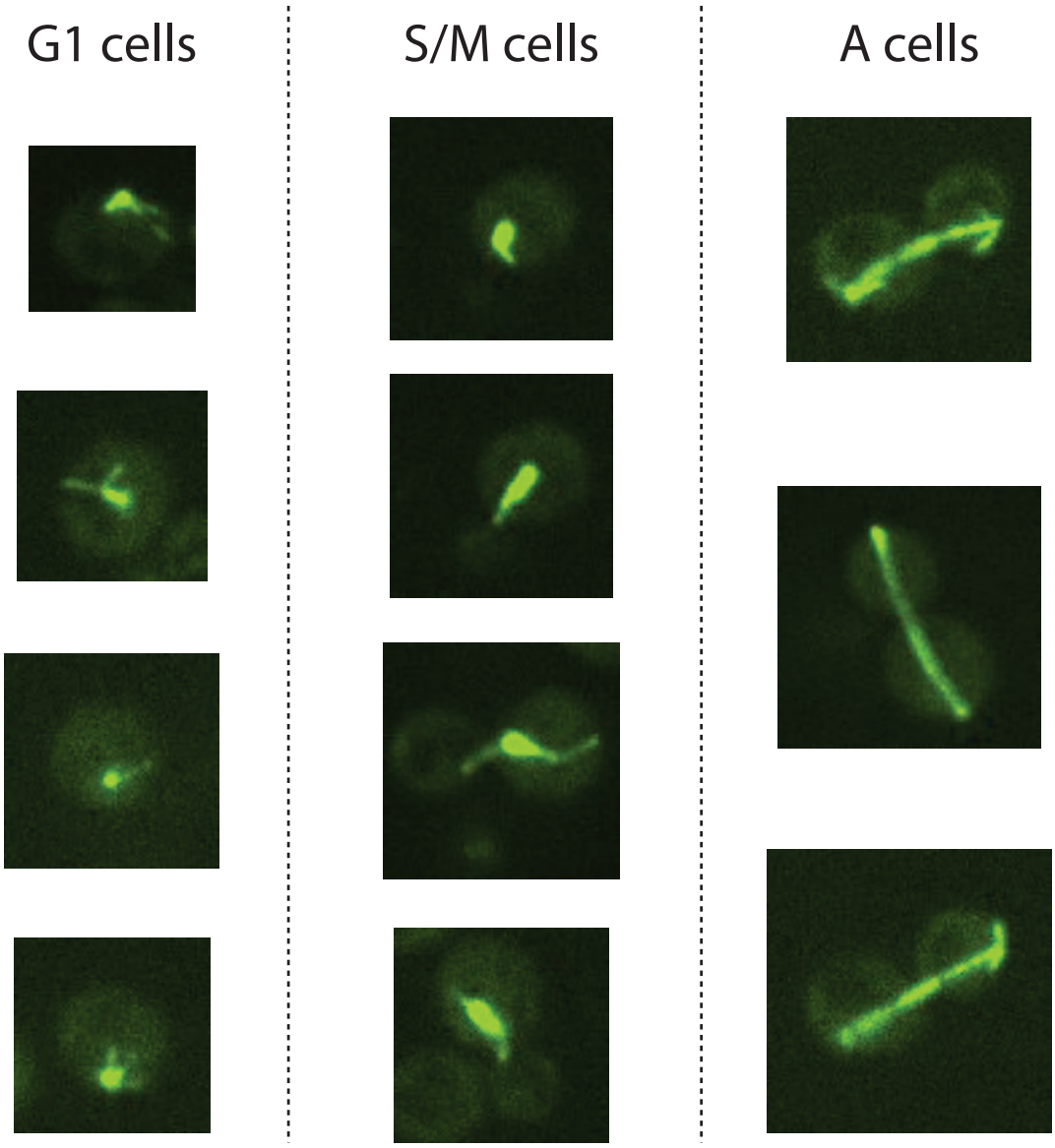

Figure S6: Typical cells in different stages of the cell cycle display different spindle shapes. G1 cells typically have a small aster. S/M cells typically have a spindle, located at the bud neck. Anaphase cells (A cells) have a long spindle extending through the cell. In order to assess accurately the phase, short movies or z-stack were taken in order to minimize the uncertainty in its determination. Detection was performed manually, and cells for which determination could not be performed accurately taken out of the analysis. We annotated the cell cycle stage of cells in Fig. 4 in different colors in order to show a display an easy readout.

***ste11*Δ background progressed beyond START prior to bursting**

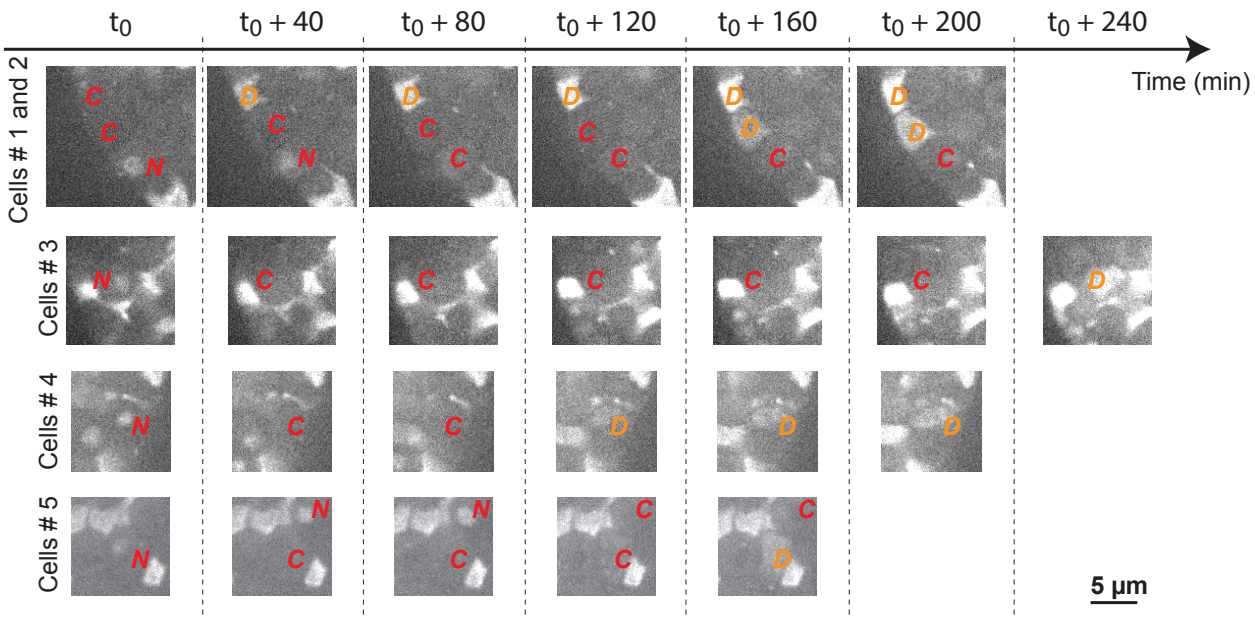

Figure S7: Montage of *ste11*Δ ; *WHI5-mCherry*a cell that died when growing under pressure. *:* N, nuclear Whi5; C cytosolic Whi5; D, cell debris. We observed instances of cells that started with nuclear Whi5 signal that became cytoplasmic, before the cell died (cells number 3 through 5). Note the transient appearance of a nuclear signal in a neighboring cell in example 5. All cells that we could track displayed a cytosolic Whi5 signal prior to death, suggesting that they had committed to the cell division cycle. Because of the low frequency and stochasticity of death events in wild-type cells, we have not been able to determine the cell cycle stage of wild-type cells that died under pressure.

Cell lysis in mutants of the CWI pathway.

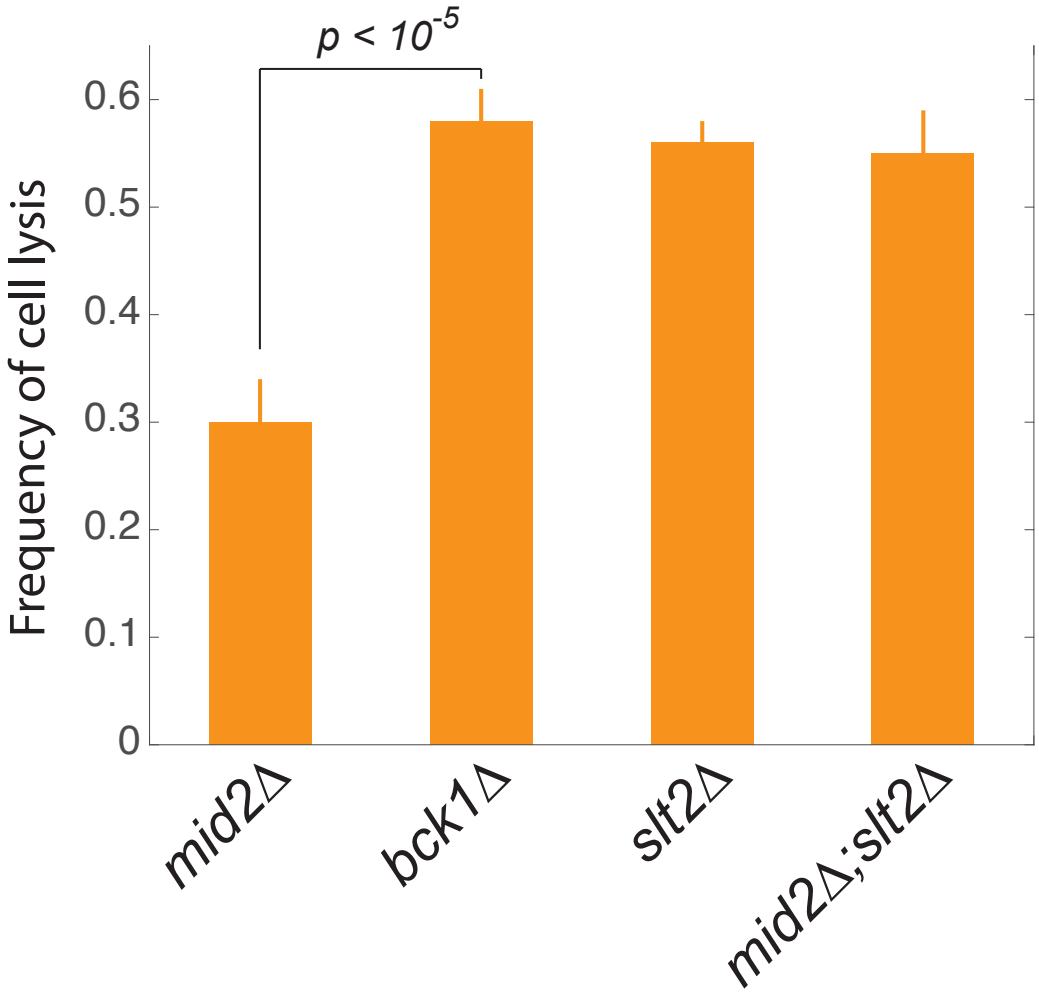

Figure S8: Fraction of cell lysis under a growth-induced pressure of 0.4 MPa, measured for various mutants in the CWI pathway. Notably, we find that a deletion of the CWI sensor Mid2 increases cell lysis to about 30% whereas a deletion of the MAPKKK *bck1*Δ or the MAPK *slt2*Δ increases cell death to about 55%; a double delete *mid2*Δ;*slt2*Δ increases cell death to the level of a *slt2*Δ, suggesting that other sensors may be activated in the CWI to signal through the MAPK Slt2p.

Cell lysis in *ste11*Δ;*slt2*Δ.

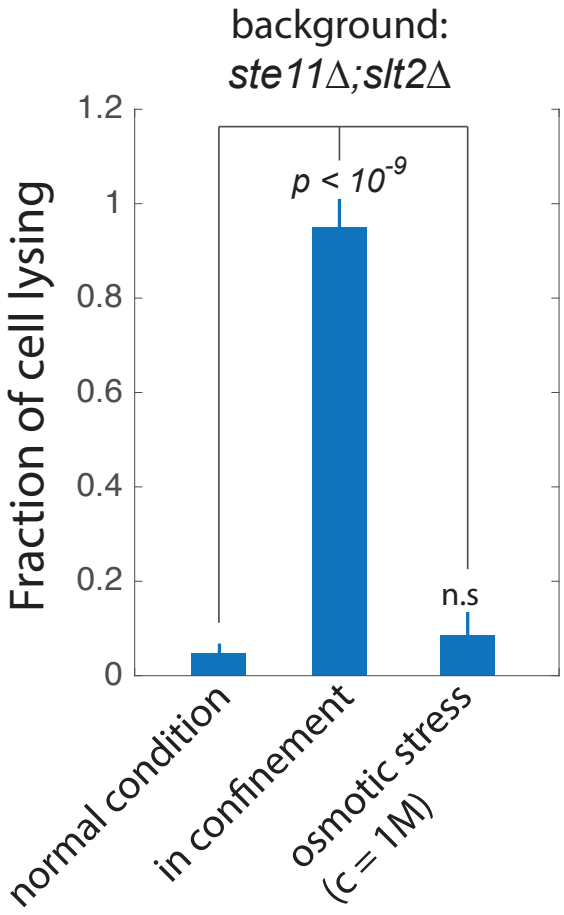

Figure S9: We measured cell lysis for *ste11*Δ;*slt2*Δ cells growing in normal conditions (SCD), in confinement in the microfluidic chamber, and under an osmotic stress of 1M. Spontaneous cell death is rarely observed in this mutant (less than 5%) and only midly increases to 8% under an osmotic stress (non-significant as compared to normal growth conditions). This is in clear contrast with growth in confinement, result in nearly all cells dying.

References

[1] M. Delarue, J. Hartung, C. Schreck, P. Gniewek, L. Hu, S. Herminghaus, and O. Hallatschek, "Self-driven jamming in growing microbial populations," *Nature Physics*, 2016.

[2] B. S. Hardy, K. Uechi, J. Zhen, and H. P. Kavehpour, "The deformation of flexible pdms microchannels under a pressure driven flow," *Lab on a Chip*, vol. 9, no. 7, pp. 935–938, 2009.